NCAR HIAPER Cloud Radar Design and Development

Pei-Sang Tsai,*E. Loew, J. Vivekananadan, J. Emmett, C. Burghart, S. Rauenbuehler**
Earth Observing Laboratory, National Center for Atmospheric Research, Boulder, Colorado

1. Introduction

HIAPER is the High-Performance Instrumented Airborne Platform for Environmental Research. This high-altitude, long-endurance Gulfstream V aircraft maintained and operated by NCAR to serve the National Science Foundations (NSF) environmental research. The Earth Observing Laboratory is currently developing the HIAPER Cloud Radar (HCR) as part of the instrumentation fleet. The development of HCR is implemented in a phased approach. A ground-based, proof-of-concept phase was completed in summer 2010. Preliminary radar design, performance and characteristics were investigated and optimized. Vertical observations and intercomparison with nearby NexRAD were also analyzed during the ground-based validation. Summer 2011, EOL is moving forward to transition HCR into airborne configuration. The initial airborne HCR will be a single polarization, W band Doppler radar. HCR is scheduled for its first test flight in March 2012. It is planned to add full polarimetric capability by December 2012 and in the future add a second wavelength operating at Ka band.

2. System Description

A block diagram of dual-channel polarimetric HCR is shown in Figure 1. The transceiver uses a two-stage up and down conversion super-heterodyne design. The first stage intermediate frequency is 156.25 MHz and the second stage is 1406.25 MHz. A 10 MHz GPS STALO is used as the system coherent source as well as the GPS location and time reference. All oscillators in the transceiver are phased locked to 125 MHz oscillator which is referenced to the 10 MHz GPS STALO. The

*Pei-Sang Tsai, E-mail: ptsai@ucar.edu

transmit waveform, generated from a waveform generator, passes through the two-stage up-conversion to give a transmit frequency 94.40625 GHz. It is then amplified by an extended interaction klystron amplifier (EIKA) to reach 1.6 kW peak power. At the front-end, a network of ferrite switches are deployed to alternate the transmit polarization and also achieve isolation between transmit and receive paths. Three ferrite switches at the output of EIKA direct the transmit power between H and V polarization to provide alternating polarization capability. Three cascaded ferrite switches in front of the LNA provide isolation during transmission. A minimum isolation of 75 dB is expected. System performance on transmit and receive paths is closely monitored using a coupler and a noise source. A portion of the transmit signal is coupled through a 40 dB waveguide coupler and attenuated to an appropriate level detectable by the crystal detector. The well-calibrated detector output indicates the power level of each pulse. The noise source is switched into the receive path periodically to monitor the receiver fluctuation and noise figure. The received signal is digitized at the rate of 125MS/s. Both in-phase and quadrature information can be archived in HCR. Standard moment products such as reflectivity, Doppler velocity and spectrum width will be provided in CFRadial format.

3. Ground Validation

HCR transceiver was configured to a ground-based, dual-antenna system in order to verify the design and performance. Figure 2 shows the ground-based configuration.Two coplanar 12-inch antennas were mounted on the top plate of a sea container. Both antennas have a matched beamwidths of $0.68°$ and gains of 46.21 dB. Custom designed antenna shrouds with millimeter-wave
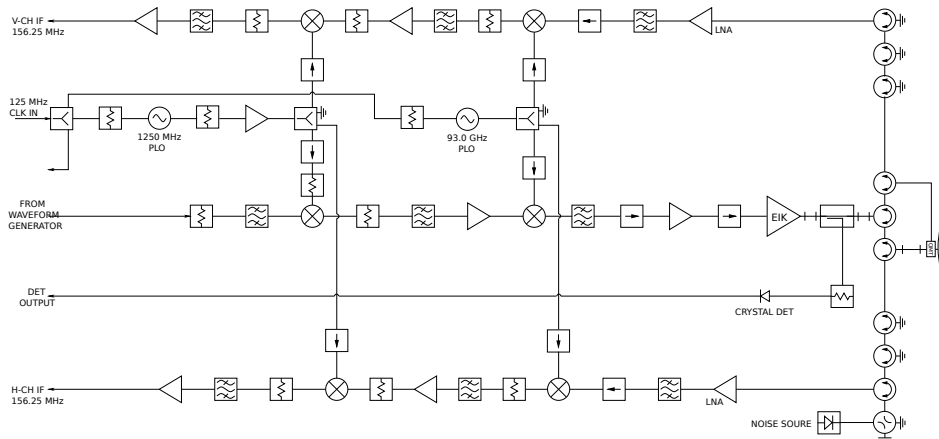
Figure 1: Block diagram of dual-channel polarimetric HCR transceiver.

Figure 2: HCR ground-based configuration.

absorber were added to provide additional isolation between transmit and receive antenna. Signal will transmit from one antenna and be received simultaneously from the other. A reflector mounted on top of both antennas can be used to steer transmit signal horizontally for desired angle. The ground configuration enabled a number of field tests for characterizing HCR radar performance. Table 1 lists the specification of the system in ground-based bistatic radar configuration.

Calibration of the system requires accurate measurements of the transmitted power, the receiver gain and noise figure. The transmit power is monitored on pulse-by-pulse basis via one of the receive channels. The signal-to-noise ratio at the input to the digitizer is 41 dB, sufficient for amplitude and phase characterization; The gain of the receiver is measured on the bench-top prior to ground-based installation and its gain was monitored periodically using the noise source calibration. The waveguide switch before the low noise amplifier in the receiver can switch between the receive antenna and a noise source. Noise source with an excess noise ratio of 20.84 dB is deployed for receiver noise figure measurement. The source equates to a thermal noise power of -86 dBm at 273K, into a 700 kHz bandwidth. The Y-factor method estimated receiver noise figure as 8.9 dB.

For ground-based calibration, a 2.375-inch trihedral corner reflector was chosen as a calibration target. The corner reflector was mounted on an adjustable fiberglass

pole located 100 m from the radar. The height of the pole can be adjusted from 3 to 7.5 m. The reflector panel was deployed to deflect antenna main beam horizontally toward the corner reflector. The expected received power is -12.3 dBm at 100m range for the trihedral corner reflector.

The maximum power recorded during calibration is -20.13 dBm. Note that there is a significant discrepancy of 8 dB between the measured power and the expected power.The 8 dB difference in estimated power is due to antenna parallax. Parallax is significant when high-gain, narrow-beam antennas are used. It is sensitive to relative antenna alignment (5). Sekelsky and Clothiaux indicate parallax can underestimate radar reflectivity in close range. The bias can be as large as -12 dB with θ_{3dB} angular offset. The theoretical calculation in is based on a single-antenna system which does not encounter antenna parallax uncertainty. Summary of HCR specification and performance are listed in Table 1.

4. NexRad Comparison

In order to compare measurements from HCR with the NexRad(KFTG) measurements from cloud with low reflectivity values were selected. This criterion ensured Rayleigh scattering for which reflectivity is independent of radar wavelength. HCR collected vertical profiles while the NexRad was operated in clear-air mode on June 1, 2010.

Figure 3 shows the KFTG reflectivity in Boulder area. The time stamp indicates the starting time of the volume scan. Since there are several tilts in every scan, the starting time of the appropriate PPI scan over Foothills lab was interpolated. The corresponding HCR vertical profile is shown in Figure 4. A band of strong echo appears at 4km height and has average reflectivity of 12.27 dBZ.

The estimated spatial resolution of the KFTG over Foothills lab is about 1.1km and the height of beam center is 3.83 km. Figure 3 shows the KFTG reflectivity in a common volume between HCR and KFTG. The corresponding HCR vertical profiles are shown in Figure 4. The lower panel of Figure 5 shows uniformly upwards velocity of 0.95 m/s. The corresponding median spectral width is 0.40 m/s. The velocity and spectral width mea-

Table 1: HIAPER Cloud Radar system performance

| Antenna Subsystem	
Type	Cassegrain
Diameter	0.3 m
Gain	46.21 dB
Beamwidth	0.68°
Transmit Frequency	94.40625 GHz
Transmitter and receiver subsystem	
Transmitter	
Type	Klystron
Frequency	94.40625 GHz
Peak Power	1.6 kW
Pulse Width	200 ns - 1μs
PRF	10 kHz
Receiver	
Noise Figure	8.9 dB
Dynamic Range	76 dB
Receiver Bandwidth	20 MHz
System Noise Power	-104 dBm
First IF	156.25 MHz
Second IF	1406.25 MHz
Sensitivity	-39.6 dBZ@1km, 0dB SNR
Unambiguous Velocity	±7.75 m/s
Dwell Time	100 ms
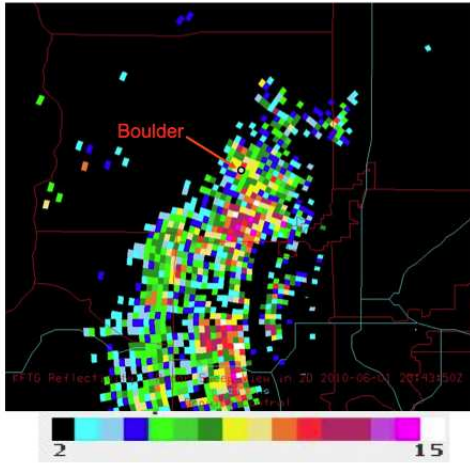
Figure 3: KFTG Reflectivity in Boulder area 23:43:50Z on June 1, 2010. Average of KFTG reflectivity values surrounding Boulder is 8.55 dBZ.
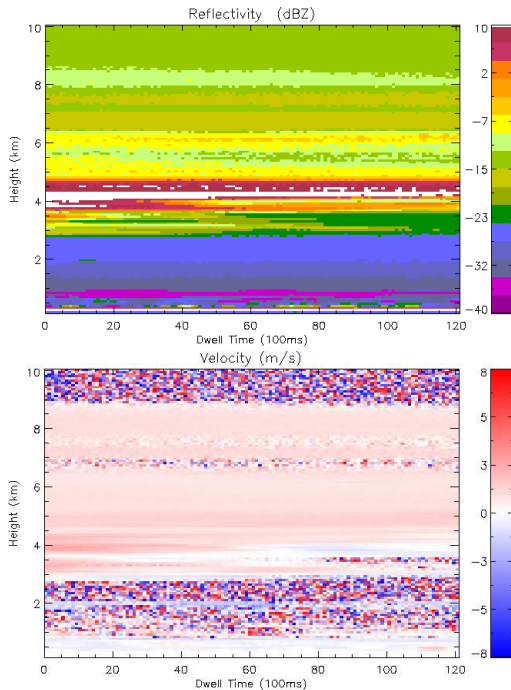

Figure 4: Vertical reflectivity (upper) and velocity (lower) profile at 23:45:07Z , June 1, 2010.

surements suggest a band of small droplets. High resolution HCR reflectivity was averaged over NexRad footprint of 1.1 km. To simulate the antenna beam characteristics, a Gaussian weighing function was applied when averaging reflectivity. The averaged HCR reflectivity varied between 3 dBZ and 7 dBZ within 12 second period. This values are in good agreement with mean NeXRad measurement of 8.55 dBZ.

5. Current Development

The ground-based HCR is reconfigured to fit inside a pod for airborne deployment. The custom designed pod is 20-inch(0.5 m) diameter and 160-inch (4.1m) in length. The pod was certified by FAA for mounting under aircraft wing The HCR in the pod is powered by an on-board power cable. An optical fiber is used for monitoring any arcing in RF circuits. Ethernet and limited signal wiring between the fuselage and the instrument payload are used for data and radar control. HCR is design to be compact to operate in the pod. The CAD model of the airborne HCR is shown in Figure 5. Four parts major sub-systems, namely, rotating reflector, a 12-inch lens antenna, a pressure vessel and the remote data system are in the pod. The pressure vessel cylinder secures the interior pressure at ground level to prevent the radar system from arcing in high altitude environment. The W-band front-end electronics, the klystron transmitter and its power supply modulator are located in the pressure vessel. Currently 67% of the space is occupied by the W-band system, the remaining 33% will be utilized for the second wavelength, Ka-band system. Subsystems such as front-end electronics and remote data system have been manufactured and tested. The integration of all subsystems are scheduled to be completed in Fall 2011.

6. Summary

This paper summarizes design and calibration of the HI-APER cloud radar. Performance of HCR was evaluated in a in ground based configuration mode using trihedral reflector and comparing reflectivity measurements in a common sampling volume with NexRAD. The preliminary
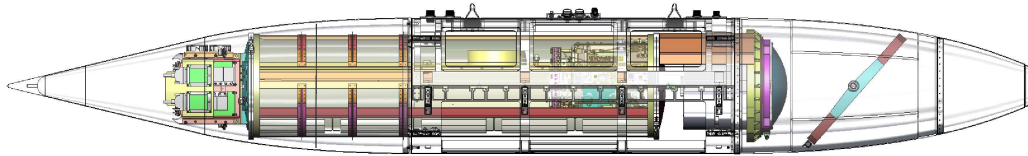
Figure 5: CAD model of the airborne HIAPER Cloud Radar.

analysis of measurements show there is a good agreement between NexRAD and HCR measurements. In a ground-based configuration the radar was operated in a bi-static mode as it used separate antenna for transmission and reception. Transceiver design and performance was optimized during ground validation. In a pod-based design a single lens antenna will be used for both transmit and reception. Ferrite switches are used for obtaining better than 75 dB isolation between receive and transmit channels. Initial airborne test of the pod-based configuration will take place in Spring 2011.

References

[1] R. J. Doviak and D. S. Zrnić. *Doppler Radar and Weather Observations*. Academic Press, second edition, 1993.

[2] R. J. Hogan, N. Gaussiat, and A. J. Illingworth. Stratocumulus liquid water content from dual-wavelength radar. *J. Atmos. Oceanic Technol.*, 22(8):1207–1218, August 2005.

[3] H. J. Liebe, G. Hufford, and M. Cotton. Propagation modeling of moist air and suspended water/ice particles at frequencies below 1000 ghz. In *Proc. of 52nd Specialists meeting of the Electromagnetic Wave Propagation Panel*, page 542. AGARD, 1993.

[4] B. E. Martner,K. A. Clark, B. W. Bartram Radar Calibration Using a Trihedral Corner Reflector *Repr. fo 31st Conf. on Radar Meteorology*, page 1028-1030

[5] S. M. Sekelsky, E. E. Clothiaux Parallax Errors and Corrections for Dual-Antenna Millimeter-Wave Cloud Radars *J. Atmos. Oceanic Technol.*, Vol.19, p478-485, April 2002

[6] F. T. Ulaby, R. K. Moore, A. K. Fung Microwave Remote Sensing, Active and Passive *Artech House, Inc.*, Volume II, 1986

[7] M. I. Skolnik Introduction to Radar Systems *McGraw Hill Pub.*, third Edition, 2001

[8] Texas Instruments. *Understanding Data Converters*, 1995. Application Report.